Earthquakes and Structures, *Vol. 9, No. 4 (2015) 767-788*
DOI: http://dx.doi.org/10.12989/eas.2015.9.4.767

Condition assessment of steel shear walls with tapered links under various loadings

Liusheng He*, Masahiro Kurata and Masayoshi Nakashima

Disaster Prevention Research Institute, Kyoto University, Gokasho, Uji, Kyoto, Japan

(Received December 4, 2014, Revised June 19, 2015, Accepted June 29, 2015)

Abstract. A steel shear wall with double-tapered links and in-plane reference was developed for assisting the assessment of the structural condition of a building after an earthquake while maintaining the original role of the wall as a passive damper device. The double-tapered link subjected to in-plane shear deformation is designed to deform torsionally after the onset of local buckling and works as an indicator of the maximum shear deformation sustained by the shear wall during an earthquake. This paper first examines the effectiveness of double-tapered links in the assessment of the structural condition under various types of loading. A design procedure using a baseline incremental two-cycle loading protocol is verified numerically and experimentally. Meanwhile, in-plane reference links are introduced to double-tapered links and greatly enhance objectivity in the inspection of notable torsional deformation with the naked eye. Finally, a double-layer system, which consists of a layer with double-tapered links and a layer with rectangular links made of low-yield-point steel, is tested to demonstrate the feasibility of realizing both structural condition assessment and enhanced energy dissipation.

Keywords: condition assessment; steel shear wall; damper; earthquake loading; low-yield-point steel

1. Introduction

Recent advances in earthquake engineering have reduced the seismic vulnerability of buildings, yet earthquake ground motions beyond those considered in design are possible as recently witnessed with the 2011 Tohoku earthquake in Japan. While the quick inspection and evaluation of building damage after major earthquake events is necessary in deciding whether to evacuate or continue normal operations, the condition assessment of structural components is not an easy task. Current post-earthquake inspection relies on trained inspectors who evaluate the condition of a building according to visual features such as cracking in concrete and residual deformations. There will be delays in inspecting buildings when many buildings are damaged by an earthquake. In recent years, structural health monitoring (SHM), which employs electric sensors and provides objective information based on engineering data, has attracted much attention. However, the application of SHM to buildings has an associated cost, including a relatively large initial investment and long-term operating fee. That said, a workable method that allows rapid condition

*Corresponding author, E-mail: liush.he@gmail.com

http://www.techno-press.org/journals/eas&subpage=7 ISSN: 2092-7614 (Print), 2092-7622 (Online)

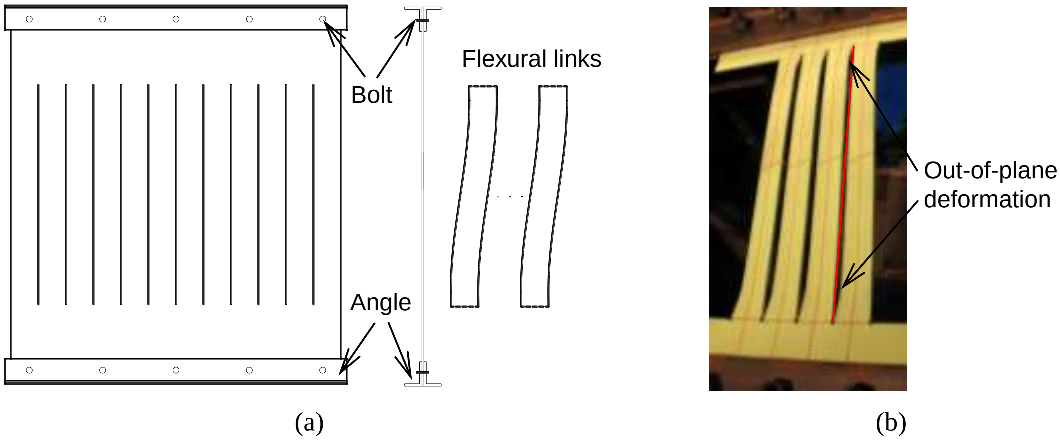

Fig. 1 Steel slit shear wall: (a) assembly illustration and (b) out-of-plane deformation of a test specimen (at a drift ratio of 5%)

assessment without extra investment is highly desirable.

Against this background, the authors adopt the concept of a hysteretic damper having the function as an SHM sensor in addition to its original function of a damper device. The realization of such a device would be expected to dramatically increase the application of SHM to standard and not just special structures. There is an interesting type of hysteretic damper called a steel slit shear wall (Hitaka and Matsui 2003, Chan and Albermani 2008, Cortes and Liu 2011, and Ke and Chen 2012), the concept of which is illustrated in Fig. 1(a). The steel slit shear wall is made of a steel panel and has a series of rectangular segments (called links) formed by laser-cutting slits. When the wall undergoes in-plane shear deformation (referred to as lateral drift hereinafter), each link behaves as a flexural member at the point of inflection located at mid-height. What attracted the authors most is the clear appearance of out-of-plane deformation at a certain level of lateral drift. By inspecting the out-of-plane deformation after an earthquake, the maximum lateral drift that the shear wall underwent can be estimated. Early attempts of implementing this idea obtained reasonable results by Jacobsen *et al.* (2010), Okamura *et al.* (2012). Although each link exhibited buckling and corresponding out-of-plane deformation involving torsional deformation, the degree of deformation was not great (Fig. 1(b)), which made it rather difficult to judge whether the wall underwent 'notable' change.

Recently, the authors proposed a steel shear wall with double-tapered links that allow for better assessment of the structural condition (He *et al.* 2013, Kurata *et al.* 2014). Fig. 2 shows one specimen tested under quasi-static cyclic loading. The segment bounded by two adjacent openings is called a double-tapered link. Under lateral drift, sequential torsional deformation in links is observed. In Figs. 2(a)-(d), the widest Link A buckles and notably deforms in torsion at a lateral drift ratio (the lateral drift divided by the link height) of 2%, Link B having mid-range width deforms at a lateral drift ratio of 2.5%, and the narrowest Link C notably deforms at a lateral drift ratio of 3.5%. The condition can be assessed as follows. If no torsional deformation is observed, the experienced maximum lateral drift must be less than 2%; if only Link A is notably deformed in torsion, the maximum lateral drift must be between 2% and 2.5%; and so forth. In this way, the maximum lateral drift experienced by the shear wall is estimated. Compared with the use of a slit wall having rectangular links, the adoption of the double-tapered shape enhances torsional

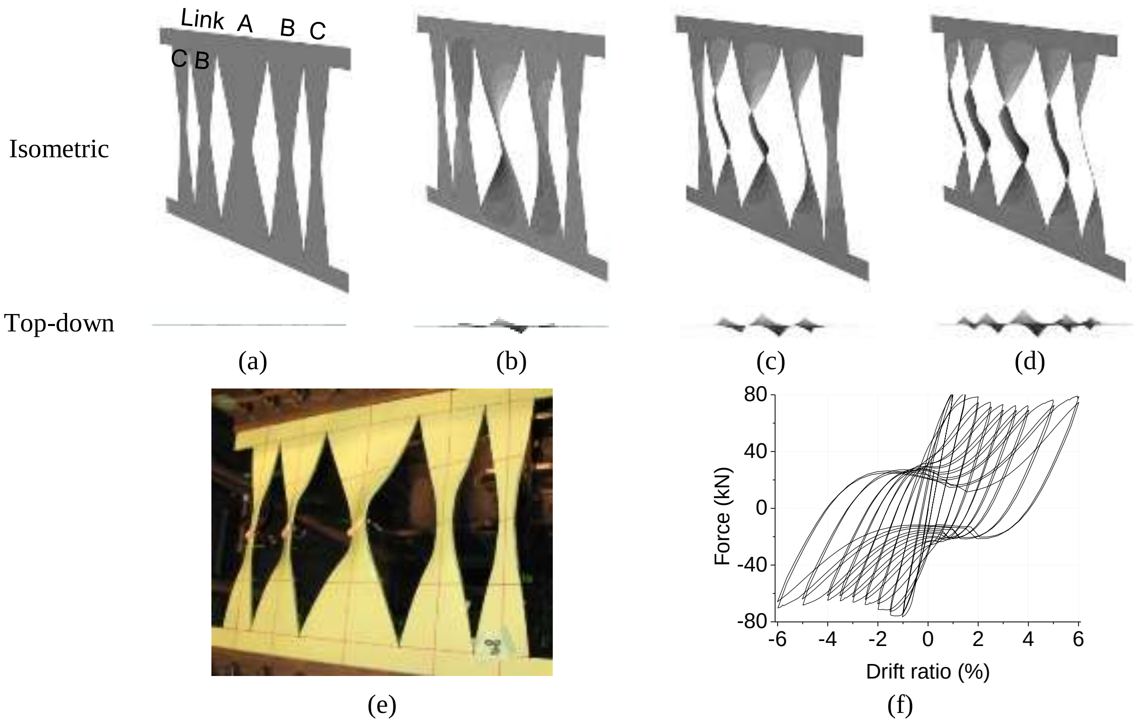

Fig. 2 Previous test: (a)-(d) diagram of torsional deformation at drift ratios of 0, 2%, 2.5% and 3.5%, respectively, (e) test specimen, and (f) hysteretic behavior (Kurata *et al.* 2014)

deformation (Fig. 2(e)). Another benefit of adopting the double-tapered links is the elimination of fracture owing to the tapering shape. Note also that the double-tapered steel component itself has already been adopted as a means of energy dissipation (Kobori *et al.* 1992, Ma *et al.* 2010).

While the early attempt of the authors to use the torsional deformation of double-tapered links for condition assessment was successful (Kurata *et al.* 2014), several aspects of the approach require improvement. One is the use of incremental two-cycle loading, a standard loading protocol commonly used in quasi-static tests, for evaluating the condition assessment capability of double-tapered links. As a primary application of double-tapered links is to monitor the maximum deformation experienced during earthquakes, condition assessment performance under earthquake loading, characterized by pseudo-random amplitudes, needs to be investigated. The other two aspects are 1) a difficulty in inspecting notable torsional deformation with the naked eye because of the existence of opening between two adjacent links and 2) pinching in hysteresis (Fig. 2(f)) because of the notable torsional deformation of double-tapered links.

The objectives of this paper are to investigate the detail of the first issue and to improve the developed steel shear wall in addressing the second and third issues. First, the effectiveness of condition assessment under earthquake loading is investigated experimentally and numerically. Initially, major dimensions of the link are determined in reference to an incremental two-cycle loading, which is considered the baseline loading protocol. The accuracy of condition assessment under various types of earthquake loadings is then examined, and the results are compared with the behavior of double-tapered links under the baseline incremental two-cycle loading. Second, new

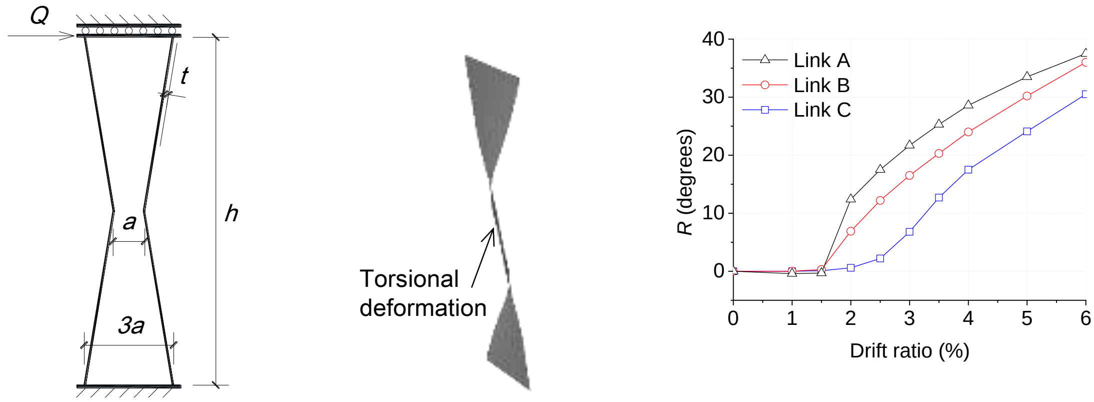

(a) (b) (c)

Fig. 3 Double-tapered link: (a) basic dimensions, (b) torsional deformation, and (c) progress of torsional deformation in terms of the rotation (R) of mid-section (Kurata *et al.* 2014)

reference links that would remain in plane under large lateral drift are added to the shear wall to enhance the objectivity of the inspection of torsional deformation of the double-tapered links. The performance of the reference links is examined in a series of tests. Finally, a double-layer system, which consists of one layer with double-tapered links and a second layer with rectangular links made of low-yield-point steel, is tested to demonstrate the feasibility of maintaining the function of structural condition assessment while enhancing the energy dissipation capacity.

2. Review of the basic behavior of the double-tapered link

A schematic of a double-tapered link under an in-plane shear force Q is illustrated in Fig. 3(a), where a, h, and t denote the mid-section width, height, and thickness of the link, respectively. While the bending moment under in-plane shear load is largest at the link ends, the link starts to yield at a location away from the ends owing to the tapering shape of the link. The location of the first yielding region is controlled by the taper rate. When the ratio of the end-section width to the mid-section width has a value of 3, the link first yields in the quarter-height regions, and the possibility of fracture at the link ends is thus low. At a large lateral drift, the quarter-height regions from the middle of the link buckle out of plane and there is notable torsional deformation, as shown in Fig. 3(b). The torsional deformation is resulted primarily from the inelastic plate buckling at quarter-height sections. The initiation and growth of torsional deformation are controlled by the width-to-thickness ratio ($\lambda = 2a/t$) but little affected by the aspect ratio ($\beta = h/2a$) as long as the link is neither too short nor too long (Kurata *et al.* 2014).

Fig. 3(c) shows the progress of torsional deformation in terms of the rotation (R) of the mid-section for the three double-tapered links in Fig. 2(a). Subjected to lateral drift following an incremental two-cycle loading protocol (Clark *et al.* 2014, ATC-24 1992, AISC 2005, and FEMA-461 2007), whose detail is presented later, the three links buckle and undergo torsional deformation at different drift ratios. The widest Link A deforms first, followed by Link B and then the narrowest Link C. Thus, by adjusting the width of the double-tapered link, local buckling and subsequent torsional deformation occur at a specifically designed lateral drift.

3. Behavior of the double-tapered link under earthquake loading

3.1 Earthquake loading

The behavior of double-tapered links under earthquake loading was evaluated using the response histories of a single-degree-of-freedom (SDOF) system subjected to various ground motions. A linear SDOF system with a natural period of 0.5 seconds and critical damping ratio of 2% was adopted to represent a low- to mid-rise steel building. The ground motions used here were taken from the ground-motion database of the PEER Transportation Research Program (PEER 2009). Ten ground motions were selected from the set of ‘broad-band’ ground motions that had a response spectrum associated with moderately large earthquakes at small distances. Ten more ground motions were selected from the set of ‘near-fault’ ground motions for sites experiencing near-fault directivity.

Fig. 4 shows the response histories of the SDOF system subjected to the 20 ground motions. The ordinate indicates the displacement, normalized by the maximum displacement, and the abscissa is the time. These displacement responses were used as the lateral drift histories in the numerical simulation presented in the next section. The 20 responses vary greatly in terms of the frequency components, the sequence of small and large peaks, and duration.

3.2 Numerical model and results under incremental two-cycle loading

The behavior of double-tapered links was examined using commercial finite element code, ABAQUS 6.10 (Dassault Systèmes 2004). For a typical story height of mid-rise steel building as 3.6 m, the height of links was determined as half the story height to double the inter-story drift. The link height was set as 360 mm for 1/5-scaled specimens to coincide with specimens used later in experiments. The links were made of conventional mild steel SS400, a Japanese steel grade equivalent to ASTM A36, and had thickness of 4.3 mm. The final parameter of the links to set was the mid-section width. Three links with mid-section widths of 30 mm (Link 1), 22 mm (Link 2) and 18 mm (Link 3) were chosen after a series of trials. The material properties were taken from tensile coupon test results. The yield stress of 374 MPa and strain hardening ratio of 0.5% were estimated for the bilinear stress-strain relationship.

In the finite element model, a three-dimensional four-node shell element with reduced integration (S4R) was used for the links. Horizontal in-plane shear displacement was applied to the top end section, while the bottom end section was clamped. A displacement associated with the first mode was imposed on the finite element model as the initial imperfection. In the direction normal to the plane of the link, the maximum imperfection amplitude of the link was scaled to 1/500 of the link height.

Fig. 5(a) shows the incremental two-cycle loading adopted as the baseline loading in this study. Fig. 5(b) shows the progress of torsional deformation in terms of the rotation (R) of the mid-sections of the three links. Clear torsional deformation of three links occurred sequentially at drift ratios of 2%, 3% and 4%. In fact, the widths of the mid-section, 30, 22 and 18 mm, were chosen such that they would exhibit notable torsional deformations at drift ratios of 2%, 3% and 4%, respectively.

3.3 Behavior of the double-tapered link under earthquake loading

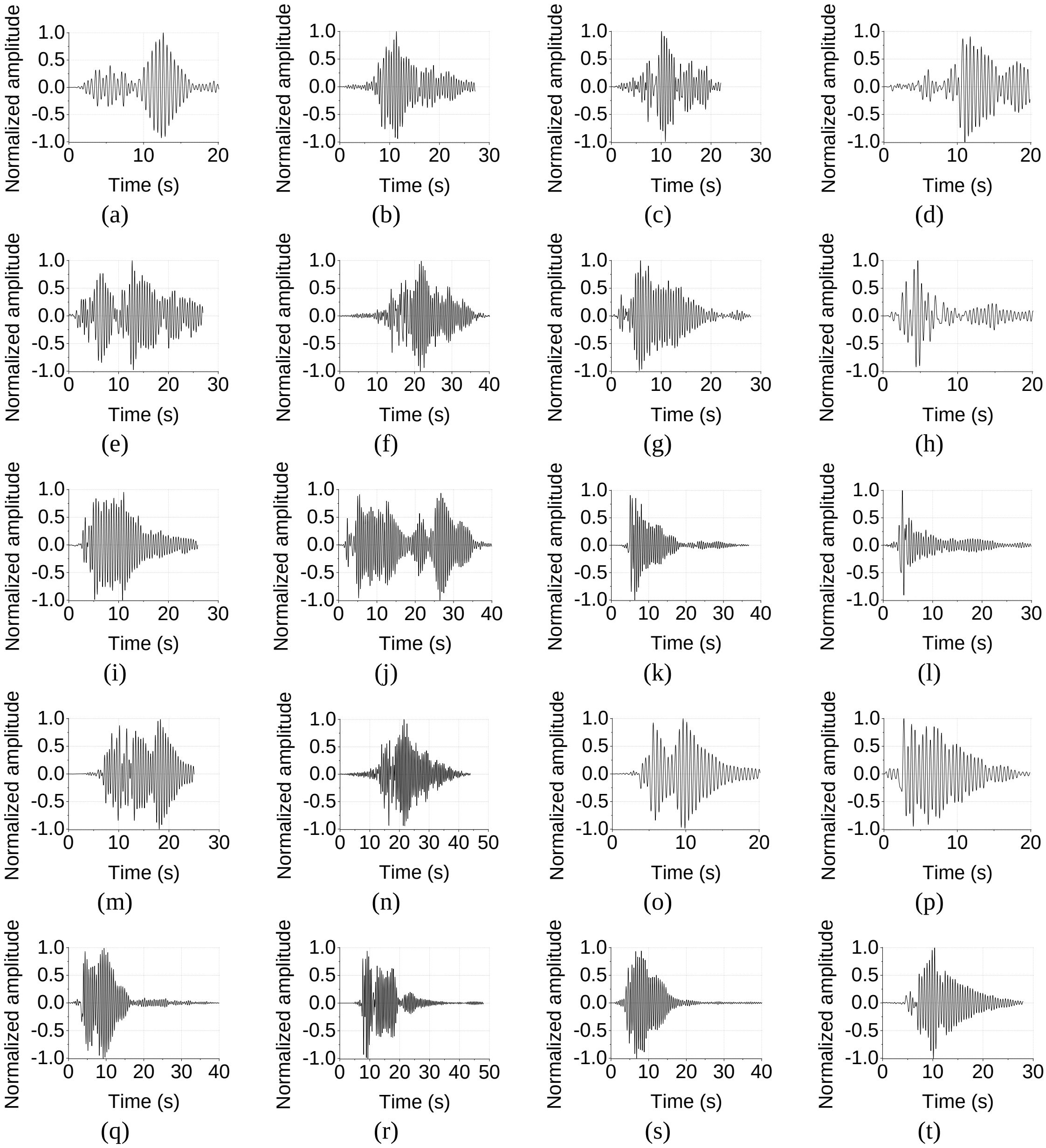

Fig. 4 Response histories under twenty ground motions

In the analysis under earthquake loading, the responses in Fig. 4 were scaled with respect to the largest peak amplitude. Each response was scaled so that the largest peak amplitude of the drift ratio was 1% to 6% in increments of 0.5% until notable torsional deformation was detected. The analysis was performed separately for Links 1, 2 and 3. The largest peak amplitude corresponding to the occurrence of torsional deformation is summarized in Fig. 6. For Link 1, the notable torsional deformation occurred at a drift ratio of 2%, which was the same result obtained under the

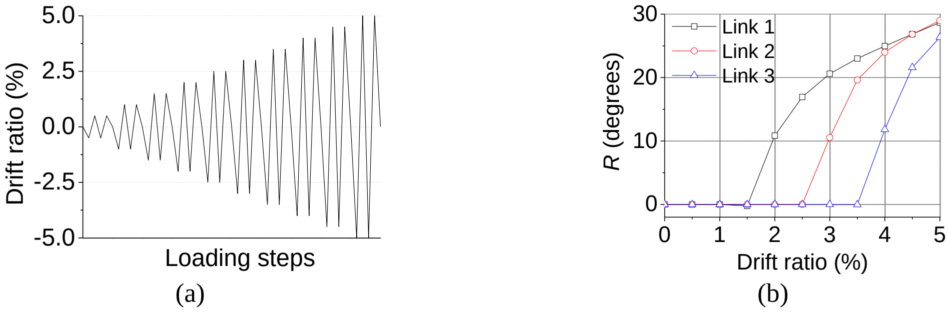

Fig. 5 Behavior under the incremental two-cycle loading: (a) loading protocol and (b) progress of torsional deformation of links with different widths

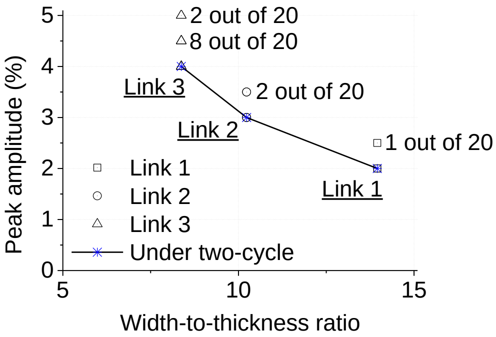

Fig. 6 Occurrence of notable torsional deformation under earthquake loading

baseline incremental two-cycle loading, except in one case (out of 20 cases) where a delay in the onset of notable torsional deformation of 0.5% (in the drift ratio) was observed. For Link 2, notable torsional deformation occurred at a drift ratio of 3%, except in two cases where there was a delay in the onset of notable torsional deformation of 0.5%. For Link 3, notable torsional deformation occurred at a drift ratio of 4% in 10 of 20 cases. Dispersion in the onset of notable torsional deformation of Link 3 was greater than that of Links 1 and 2, with a delay in the onset of notable torsional deformation of 1% in two cases and a delay of 0.5% in eight cases.

The analysis results (i.e., the drift ratios corresponding to notable torsional deformation) under earthquake loading were mostly consistent with those under the baseline incremental two-cycle loading for Links 1 and 2. Dispersion in the onset of notable torsional deformation was greater for the narrower links, whose torsional deformations became notable at larger drift ratios. Furthermore, the errors were always on the conservative side in that the drift ratio for notable torsional deformation was larger than the target drift ratio. Note also that errors arose for loadings with relatively few large peaks especially around the largest peak. However, the vast majority of data had error ratios, defined as the difference relative to the target drift ratio, within 25%. The level of accuracy expected for the proposed condition assessment is naturally not so high (as it resorts to inspection with the naked eye), and most likely distinction between maximum story drifts of 1% and 2% or at most distinction among maximum story drifts of 1%, 1.5%, or 2% is what is expected in this assessment. For instance, by adding a rigid zone whose total height is as great as the link's height, the link's drift ratios of 2% and 4% correspond to story drift ratios of 1%

and 2%, respectively. Considering the level of expected accuracy and especially the pseudo-random nature of earthquake loading, an error ratio of 25% for a very limited number of cases is deemed acceptable. To summarize, the baseline incremental two-cycle loading was judged to be sufficient in the design of double-tapered links, given the small variations in different earthquake responses.

4. Addition of in-plane reference

Although the torsional deformation was notable in the previous test (Fig. 2(e)), the diamond-shape opening between adjacent double-tapered links introduced difficulty in the recognition of notable torsional deformation with the naked eye. To reduce error in visual inspection, the addition of a reference that remains in plane between the double-tapered links was found to provide a solution.

Two types of in-plane references were proposed. Fig. 7(a) shows the first type, called the 'wing' type. Two wings were added at the mid-section and narrow rectangular strips were placed adjacent to the double-tapered link. The narrow rectangular strip was designed to maintain in-plane behavior until very large deformation. As the mid-region remained elastic, the wing with a narrow design (i.e., width of 20 mm) did not affect the basic behavior of the double-tapered links. In the previous study (Kurata *et al.* 2014), the 'off-one-thickness' criterion for notable torsional deformation was defined as the instant when the out-of-plane displacement at the edges of the quarter-height sections exceeded one thickness of the double-tapered link. With the introduction of wings and rectangular strips, the closeness between the wing and reference allows easier recognition of torsional deformation after the double-taped link buckles. Here, the off-one-

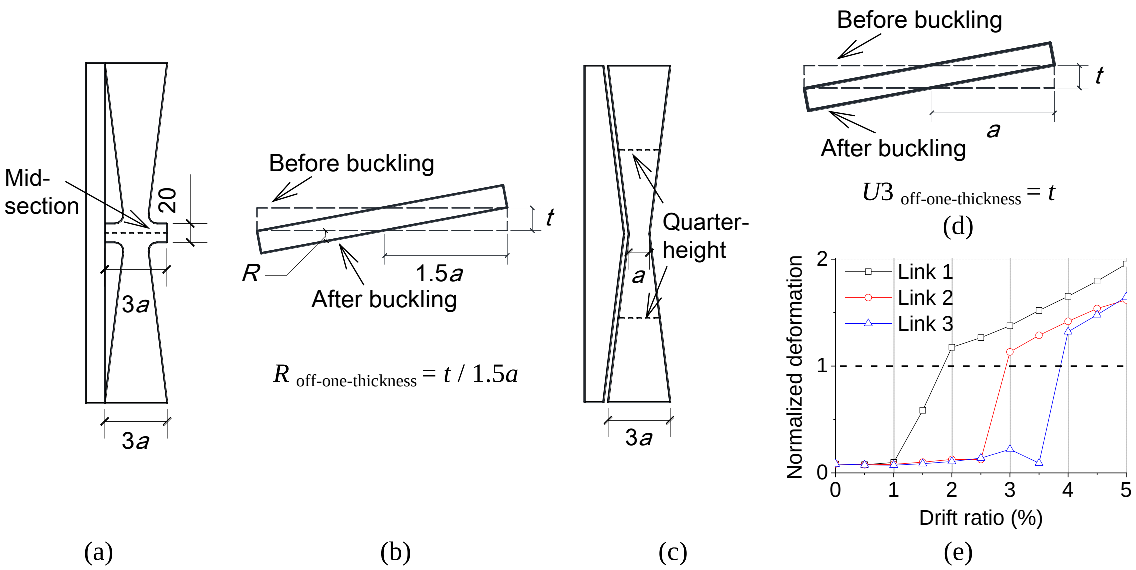

Fig. 7 Addition of in-plane reference: (a) 'wing' type, (b) off-one-thickness at the mid-section, (c) 'whole-height' type, (d) off-one-thickness at the quarter-height section, and (e) progress of the out-of-plane deformation

thickness criterion is applied at the mid-section where the wing is added. When the out-of-plane deformation at the edge of the wing is larger than the thickness of the link, the torsional deformation is considered notable as shown in Fig. 7(b).

Fig. 7(c) shows the second type, called the 'whole-height' type, placed next to the double-tapered link. The reference that is of a shape of diamond was also intended to remain in plane until very large deformation as the width at the ends was set to be small (as small as the width of the wing-type reference link in Fig. 7(a)). The closeness between the edges of the reference and double-tapered link along the whole height makes visual inspection even easier. For this type of reference, the out-of-plane displacement at the quarter-height section, the section that first buckles and undergoes increasing torsional deformation, is adopted as the reference point. As a reference is available at the quarter-height section, the most direct out-of-plane displacement ($U3$) in that section is adopted for the judgment of off-one-thickness, as shown in Fig. 7(d). For the three double-tapered links shown in Fig. 5(b), the progress of normalized out-of-plane deformation (out-of-plane displacement divided by plate thickness) at quarter height is shown in Fig. 7(e). Notable torsional deformation of Links 1, 2 and 3 was recognized at drift ratios of 2%, 3% and 4%, respectively, as the normalized deformation became larger than unity.

5. Enhancement of energy dissipation

The authors' previous work placed more emphasis on the condition assessment rather than on the energy dissipation of double-tapered links. However, as shown in Fig. 2(f), the relatively thin plate designed to have early and large torsional deformation exhibited significant pinching in its hysteretic curve. Another objective of the present paper is to reduce pinching and thus enhance energy dissipation while maintaining the function of condition assessment.

Rectangular links can be designed to dissipate energy in a stable manner when a proper value is selected for the width-to-thickness ratio. Thus, a shear wall with a combination of rectangular links and double-tapered links seems to be a practical solution. However, rectangular links are susceptible to early fracture at the link ends, which reduces their strength and energy dissipation (Hitaka and Matsui 2003, Chan and Albermani 2008, Cortes and Liu 2011). To eliminate fracture at the ends of rectangular links, the use of a low-yield-point steel with large strain hardening, both kinematic and isotropic, and large elongation capacity was considered. The application of low-yield-point steel to shear walls is not new (Nakashima *et al.* 1994, 1995, Chen and Jhang 2006), but there has been little work on the application of such steel to slit shear walls. Fig. 8 shows the stress-strain relationships of SS400 and LYP100, a low-yield-point steel with a nominal yield stress of 100 MPa. As compared with SS400, LYP100 is characterized by low initial yield stress and large strain hardening. These properties allow for early material yielding starting from a small lateral drift and ensure good deformation capacity.

6. Preparation of tests

6.1 Test specimens

In this study, five specimens were designed. Specimens 1 to 4 were made of SS400 and had double-tapered links with the same dimensions as those in the previous simulation. Specimen 5 was a combination of double-tapered links made of SS400 and rectangular links made of LYP100.

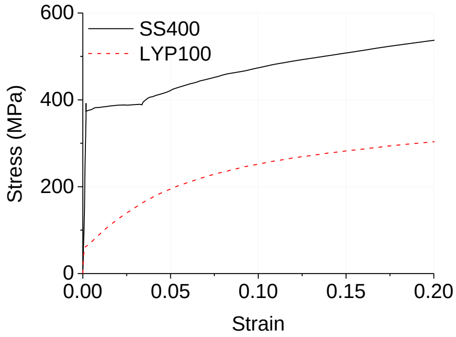

Fig. 8 Stress-strain relationship of the low-yield-point steel

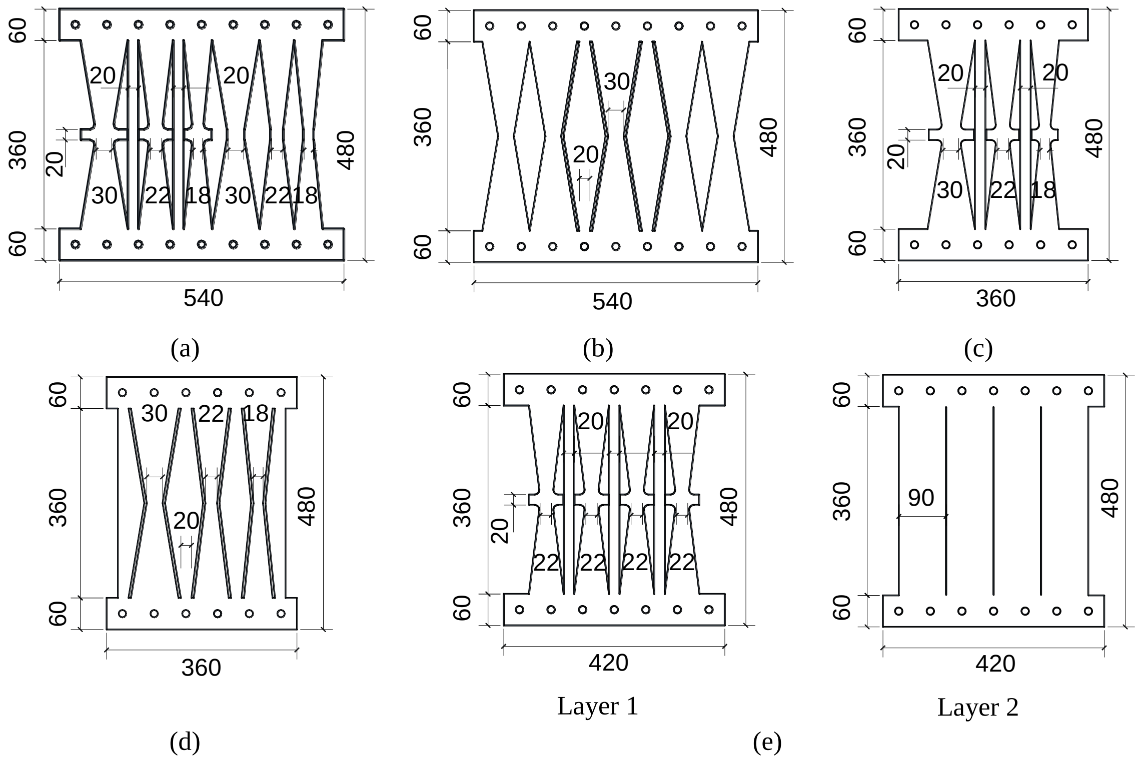

Fig. 9 Dimensions of specimen (unit: mm): (a)-(e) Specimens 1-5

Fig. 9 shows the dimensions of each specimen in detail. Specimens 1 and 2 were used to examine the occurrence of notable torsional deformation for links with different widths and the effectiveness of the in-plane reference. Specimen 1 had three types of double-tapered links, half of which had the wing-type reference. Specimen 2 had four identical double-tapered links with a mid-section width of 30 mm, where one link was bounded by the whole-height-type reference. Both types of reference had an end-section width of 20 mm, giving a small width-to-thickness ratio of 4.4 that ensured in-plane behavior. The gap between the wing and reference was 3 mm, and the slit width between the whole-height-type reference and the double-tapered link was 5 mm. The small gap and slit width ensured the close separation of the double-tapered link and reference. Specimens 3 and 4 were used to investigate the behavior of double-tapered links under earthquake loading. With both specimens featuring three different double-tapered links, Specimen 3 had the wing-type reference and Specimen 4 had the whole-height-type reference. Specimen 5 was an assembly of two layers, Layer 1 with double-tapered links for condition assessment and Layer 2 with rectangular links for energy dissipation. Layer 1 had four identical double-tapered links with the wing-type reference and a mid-section width of 22 mm. Layer 2 had four identical rectangular links divided by vertical slits with a slit width of 0.5 mm. Fig. 10 shows how Specimen 5 was assembled. The two layers were placed in parallel and separated by a 9-mm-thick steel plate spacer, which allowed the two layers to behave without interference.

Each specimen had top and bottom portions beyond the double-tapered links. These portions had a depth of 60 mm and holes for connection to the loading frame. Double-sided angles and high-strength bolts were used.

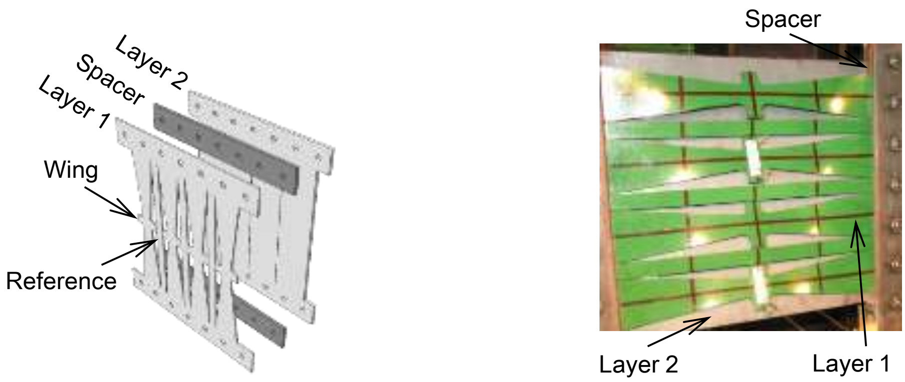

(a) (b)

Fig. 10 Assembly of Specimen 5: (a) overview and (b) test specimen

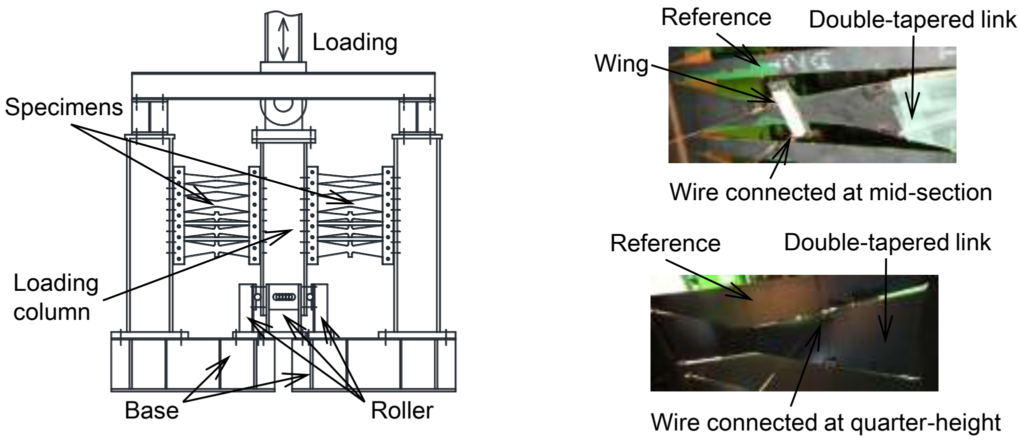

(a) (b)

Fig. 11 Test setup: (a) specimen installation and (b) measurement of torsional deformation

6.2 Test setup and instrumentation

The specimen was installed with a rotation of 90° in a steel frame consisting of three wide-flange columns (H-250×250×9×14 mm) as shown in Fig. 11(a). The two exterior columns were securely posted on the base frame, while the middle column was attached to a vertical jack and moved vertically. To orient the middle column vertically, both ends of the middle column were clamped by restrainers and rollers. Two identical specimens were installed as one pair, with one specimen installed on each side of the middle column to check the variability of the two seemingly identical specimens. The drift ratio (i.e., the shear displacement) of the specimen was controlled by the measurement of the vertical displacement of the middle column, and the shear force applied was measured by a load cell attached to the vertical jack. The shear force applied to each specimen was taken to be half the force measured by the load cell.

The out-of-plane deformation and torsional deformation of links were measured as shown in Fig. 11(b). For specimens with the wing-type reference, two wires were connected to the wing perpendicular to the plane of the link, with the other ends of the two wires connected to two displacement transducers. For specimens with the whole-height-type reference, two wires were connected to the edge at quarter height perpendicular to the plane of the link, with the other ends of the two wires connected to two displacement transducers.

6.3 Loading protocol

The baseline incremental two-cycle loading was the same as that in the simulation (Fig. 5(a)). For the earthquake loading, two (Fig. 4(f) and (g)) out of the 20 responses in Fig. 4 were selected as representative loading histories. To reduce the loading time under earthquake loading, the cycles with amplitudes smaller than 20% of the largest peak amplitude were considered to make little contribution to the torsional deformation and were therefore omitted. It was verified by numerical simulation that such omission did not affect torsional deformation. The actually adopted loading histories are shown in Fig. 12. The largest peak amplitude in Fig. 12(a) is located around the middle of the history, and there are many pre-peak and post-peak cycles of small amplitudes. This loading was designated as the 'middle-peak' earthquake loading. In Fig. 12(b), the largest peak amplitude is early in the history and is followed by decaying amplitudes; this loading was called 'early-peak' earthquake loading. The middle-peak earthquake loading, early-peak earthquake loading and baseline incremental two-cycle loading having steadily increasing amplitudes were notably different from each other in terms of the sequence toward the largest peak amplitude. Table 1 summarizes the loading protocols adopted for respective specimens.

Table 1 Loading sequence

Specimen	Loading protocol	Detail
1	Incremental two-cycle	Fig. 9(a)
2	Incremental two-cycle	Fig. 9(b)
3	'Middle-peak' earthquake	Fig. 9(c)
4	'Early-peak' earthquake	Fig. 9(d)
5	Incremental two-cycle	Fig. 9(e)

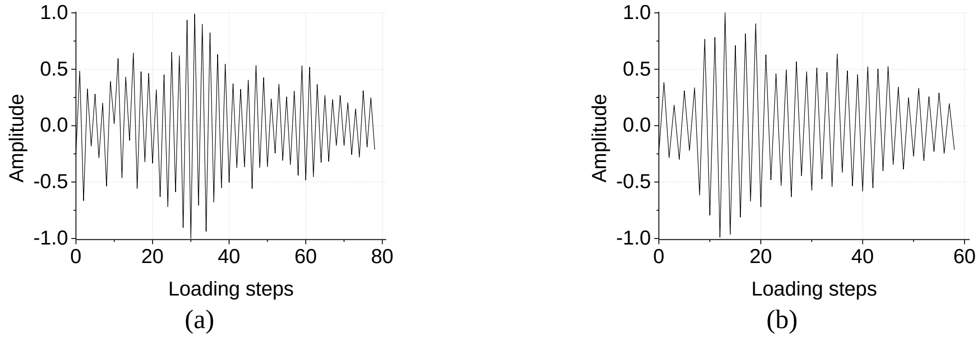

Fig. 12 Adopted earthquake loading: (a) 'middle-peak' and (b) 'early-peak'

7. Test results

7.1 Performance of condition assessment under the incremental two-cycle loading

7.1.1 Specimen 1 with the wing-type reference

Specimen 1 had double-tapered links with and without wing-type references (Fig. 13(a)). At a drift ratio of 2.5%, only the widest Link 1 showed notable torsional deformation (marked with a red circle), while the other two links remained mainly in plane (Fig. 13(b)). At a drift ratio of 3.5%, Link 2 with mid-range width exhibited notable torsional deformation (marked with a red circle), the widest Link 1 deformed further, but the narrowest Link 3 remained mainly in plane (Fig. 13(c)). At a drift ratio of 4.5%, the narrowest Link 3 exhibited notable torsional deformation (marked with a red circle), and Links 1 and 2 deformed further (Fig. 13(d)). With wings and reference strips, the judgment of notable torsional deformation was more accurate and easier than that in double-tapered links without references originally studied in the preceding paper (Kurata *et al.* 2014).

Fig. 13(e) shows the progress of torsional deformation in terms of rotation (R) of the mid-section; solid curves are results for the left specimen and dashed curves are those for the right specimen. The horizontal dashed lines correspond to the rotation angles when off-one-thickness out-of-plane deformation occurs. As illustrated in Fig. 11 for the test setup, two identical specimens were loaded simultaneously. The two specimens exhibited very close behavior, which indicated that the addition of wings did not influence the progress of torsional deformation and the finding from the preceding paper still holds. According to the off-one-thickness criterion, notable torsional deformation occurred at drift ratios of 2.5%, 3.5% and 4.5% successively.

Compared with the simulation (Fig. 5(b)), the occurrence of notable torsional deformation in the test was delayed consistently by a drift ratio of 0.5%. This was attributed to a decrease in fixity at the boundary conditions. The connection part of the double-tapered links was sandwiched by two angles on either side using high-strength bolts, and the angles were bolted to the loading column. Under large lateral drift, the ends of the links were subjected to large tension and compression stress, which somewhat reduced the thickness of the connection part according to Poisson's ratio and thus the friction force around the bolt holes. Such reduction of fixity allowed slight rotation at the link ends, which eventually delayed the torsional deformation. Note that such delay was not observed in the previous study (Kurata *et al.* 2014), in which there was a band zone between the connection part and link ends (Fig. 2(e)). This band zone most likely provided a buffer

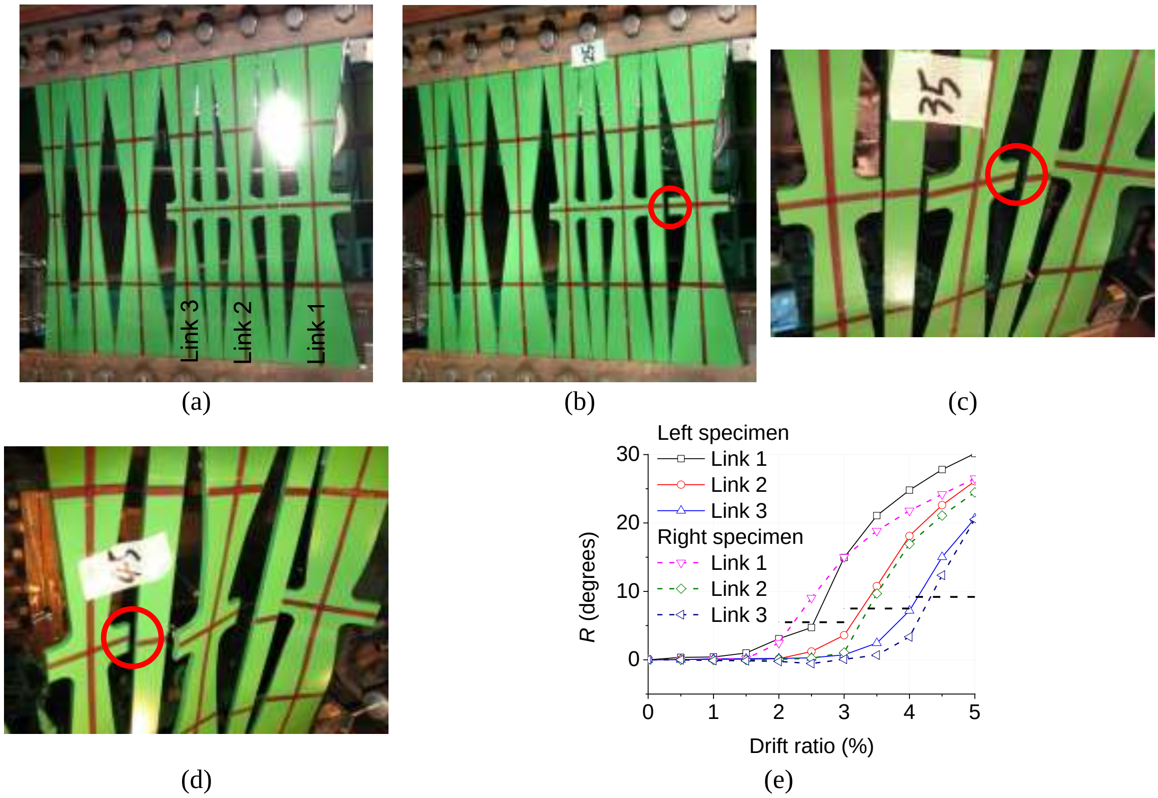

Fig. 13 Specimen 1 with the wing-type reference: (a) before loading, (b) at a drift ratio of 2.5%, (c) enlarged view at a drift ratio of 3.5%, (d) enlarged view at a drift ratio of 4.5%, and (e) progress of torsional deformation

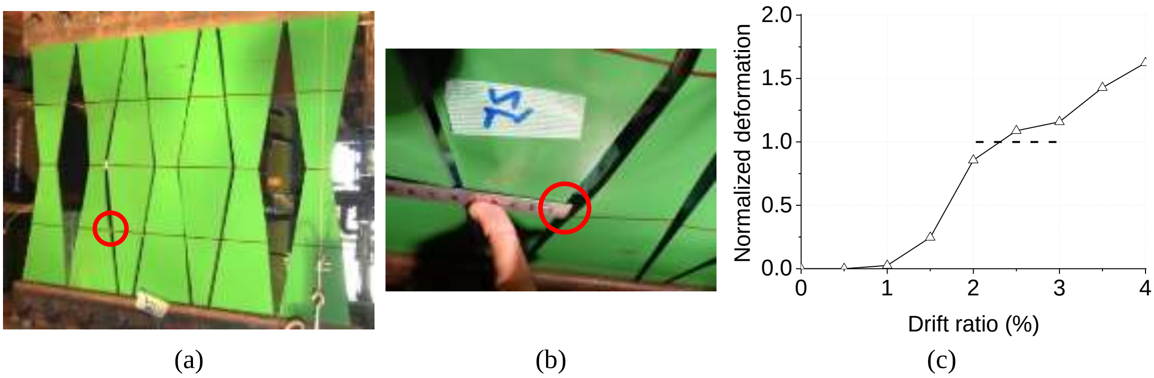

Fig. 14 Specimen 2 with the whole-height-type reference: (a) at a drift ratio of 2.5%, (b) enlarged view at a drift ratio of 2.5%, and (c) progress of out-of-plane deformation at the quarter-height section

of the large stresses between the link ends and connection part, and guaranteed more reliable fixity. As discussed in a previous section, a difference of 0.5% in the drift ratio is considered acceptable error in the light of practical application.

7.1.2 Specimen 2 with the whole-height-type reference

Specimen 2 had four identical double-tapered links whose dimensions were the same as those of Link 1 in Specimen 1. At a drift ratio of 2.5%, there was notable out-of-plane deformation at the edge of the quarter-height section (marked with a red circle) as shown in Fig. 14(a) and (b). Inspection of notable torsional deformation was easier and more objective with the reference. Fig. 14(c) shows the progress of normalized out-of-plane deformation at the edge of the quarter-height section. The normalized out-of-plane deformation exceeded unity at a drift ratio of 2.5%, which met the off-one-thickness criterion. The occurrence of notable torsional deformation was the same as that for Link 1 in Specimen 1.

7.2 Performance of condition assessment under earthquake loading

The test results under the baseline incremental two-cycle loading showed that three links deformed notably at drift ratios of 2.5%, 3.5% and 4.5% sequentially. Thus, the largest peak amplitudes of earthquake loading in Fig. 12 were scaled to drift ratios of 1.5%, 2.5%, 3.5% and 4.5% respectively. Specimens 3 and 4 were loaded under these four loadings sequentially.

7.2.1 Specimen 3 with the wing-type reference

Specimen 3, having three double-tapered links (Links 1, 2 and 3) with the wing-type reference (Fig. 15(a)), was subjected to the middle-peak earthquake loading. At the largest peak drift ratio of 1.5%, the three links remained in plane without torsional deformation. Notable torsional deformation of the three links occurred at the largest peak drift ratios of 2.5%, 3.5% and 4.5% sequentially, from the widest Link 1 to the narrowest Link 3. The wing-type reference remained in plane throughout the entire loading and made the torsional deformation very notable (marked with red circles), as shown in Fig. 15(b).

Fig. 16 shows the histories of torsional deformation in terms of the rotation (R) of the mid-section. At the largest peak drift ratio of 1.5%, all three links remained in plane with nearly zero rotation (Fig. 16(a)); then, at the largest peak drift ratio of 2.5%, Link 1 met the off-one-thickness criterion and the other two links remained mainly in plane (Fig. 16(b)); next, at the largest peak drift ratio of 3.5%, Link 2 met the off-one-thickness criterion (Fig. 16(c)); finally, at the largest

(a) (b)

Fig. 15 Specimen 3 under earthquake loading: (a) before loading and (b) at the largest peak drift ratio of 4.5%

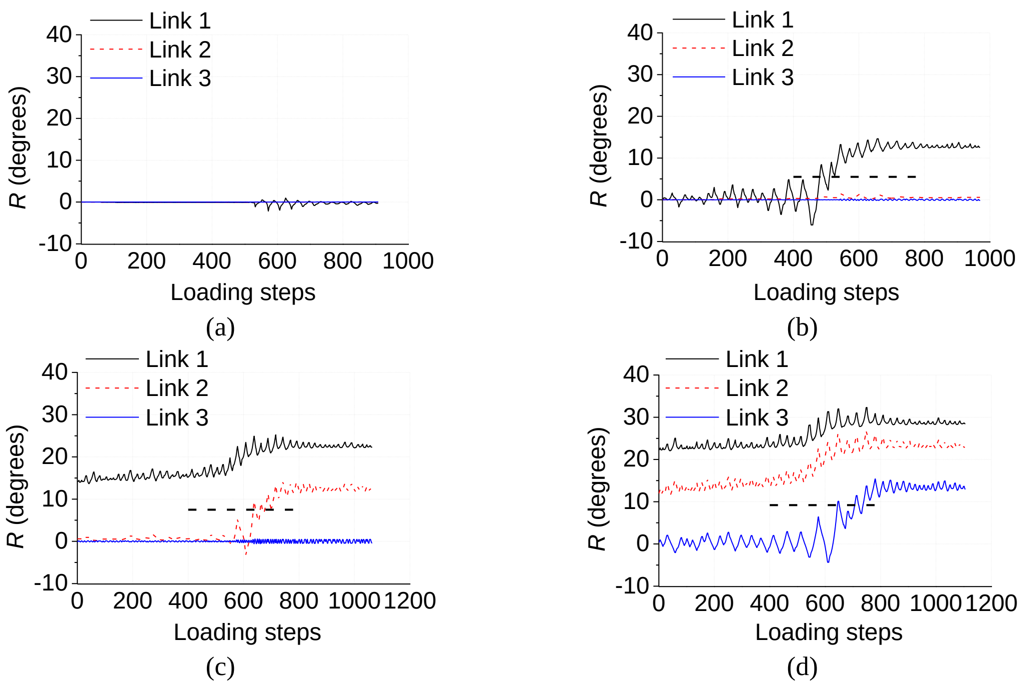

Fig. 16 Progress of torsional deformation of Specimen 3: (a)-(d) at the largest peak drift ratios of 1.5%, 2.5%, 3.5% and 4.5%, respectively

peak drift ratio of 4.5%, Link 3 met the off-one-thickness criterion, and Links 1 and 2 deformed further (Fig. 16(d)).

7.2.2 Specimen 4 with the whole-height-type reference

Specimen 4 had three double-tapered links (same as Specimen 3) and was subjected to the middle-peak earthquake loading. The whole-height-type reference (Fig. 17(a)) was adopted for this specimen. At the largest peak drift ratio of 1.5%, out-of-plane deformation at the quarter-height sections was very small and barely recognizable. At largest peak drift ratios of 2.5%, 3.5% and 4.5%, the off-one-thickness criterion was recognized in visual inspection. The whole-height-type reference remained in plane throughout the entire loading and made the torsional deformation notable (marked with red circles), as shown in Fig. 17(b).

Fig. 18 shows the histories of normalized out-of-plane deformations at the quarter-height section. At the largest peak drift ratio of 1.5%, Link 1 buckled out of plane, but the normalized deformation was smaller than unity, which did not meet the off-one-thickness criterion. At the largest peak drift ratio of 2.5%, the normalized deformation of Link 1 exceeded unity, and notable torsional deformation was confirmed. At largest peak drift ratios of 3.5% and 4.5%, the normalized deformation of the other two links met the off-one-thickness criterion.

Both types of reference remained in plane throughout the loading and worked effectively. As a shear wall configured with double-tapered links and a whole-height-type reference can be manufactured easily by cutting continuous slits in a steel plate, the whole-height-type reference is considered easier to implement.

Under each of the two earthquake loading tests, notable torsional deformation was recognized

Fig. 17 Specimen 4 under earthquake loading: (a) before loading and (b) at the largest peak drift ratio of 4.5%

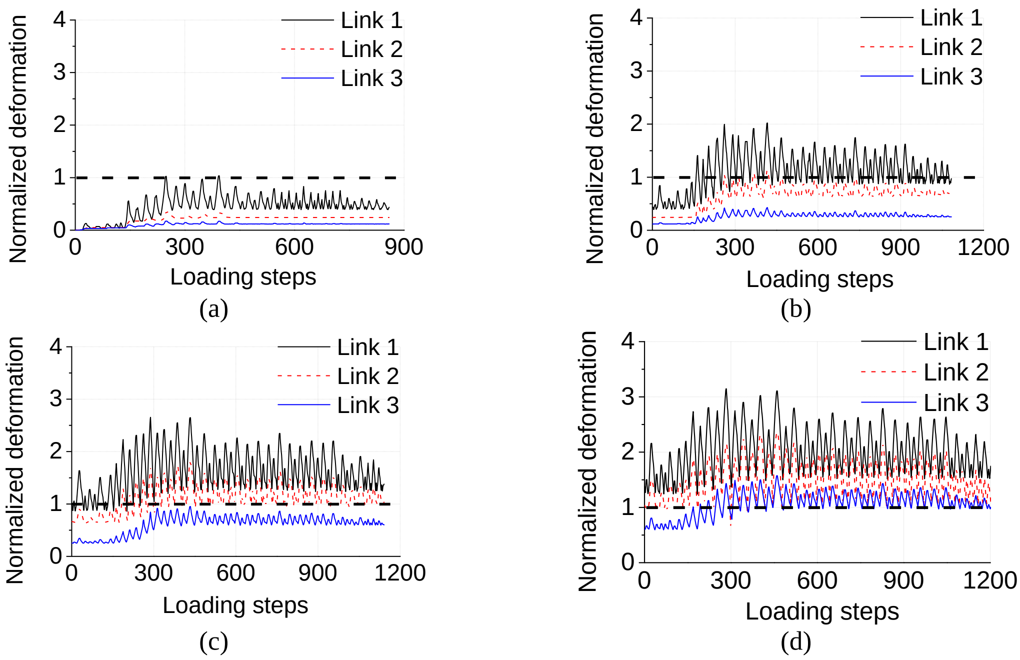

Fig. 18 Progress of out-of-plane deformation at the quarter-height section of Specimen 4: (a)-(d) at the largest peak drift ratios of 1.5%, 2.5%, 3.5% and 4.5%, respectively

at the largest peak amplitude that was the same as that achieved by the baseline incremental two-cycle loading. This indicated that the occurrence of notable torsional deformation was primarily controlled by the largest peak amplitude. Cycles before the largest peak contributed to the in-plane plastic deformation but did not trigger the notable torsional deformation. Note that, once torsional deformation becomes notable, further increase of the torsional deformation with following cycles (appeared not significant in tests) does not matter for the judgment. Despite the pseudo-random nature of earthquake loading, the baseline incremental two-cycle loading was verified as a good representative in determining the occurrence of notable torsional deformation.

7.3 Dual-function double-layer system

Specimen 5 was a combination of double-tapered links and rectangular links, and was designed to be a feasible system for both condition assessment and enhanced energy dissipation.

7.3.1 Performance of condition assessment

Layer 1 of Specimen 5 had four identical double-tapered links for condition assessment. Torsional deformations of two links, one in the middle and the other at the edge, were measured. Fig. 19 shows the progress of torsional deformation in terms of the rotation (R) of the mid-section. The two links underwent very similar torsional deformations. With the links having the same

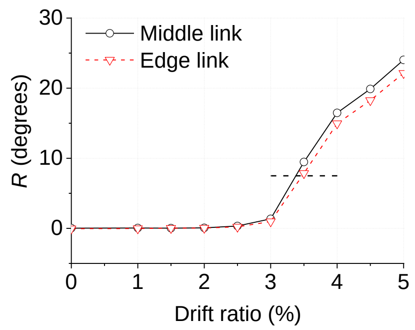

Fig. 19 Progress of torsional deformation of double-tapered links

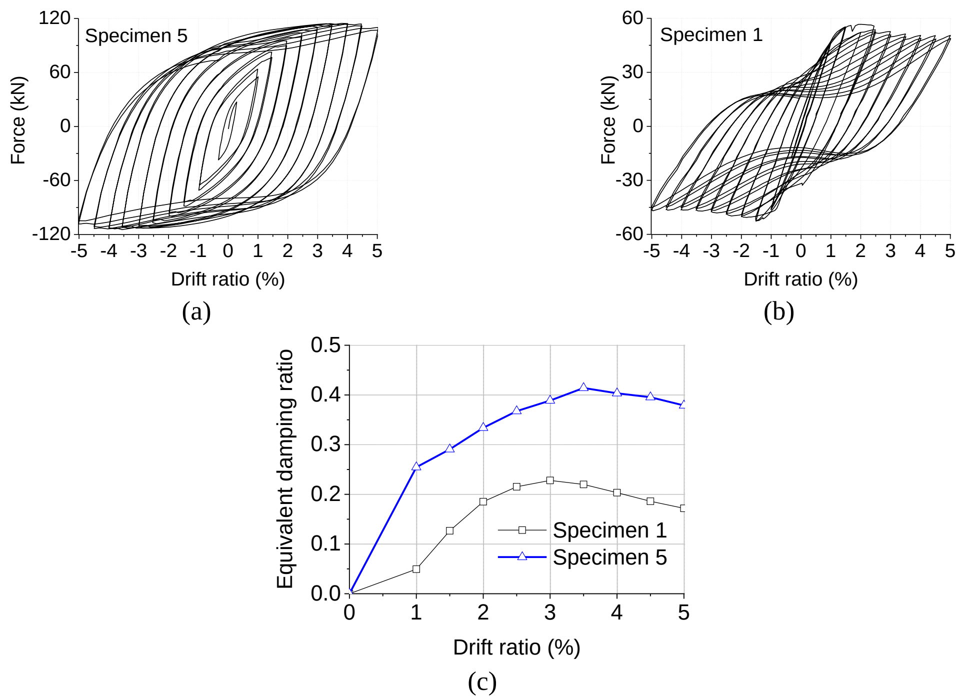

Fig. 20 Hysteretic curve and equivalent damping ratio: (a) hysteresis of Specimen 5, (b) hysteresis of Specimen 1, and (c) equivalent damping ratios

dimensions as Link 2 in Specimen 1, notable torsional deformation occurred at the same drift ratio of 3.5%.

7.3.2 Hysteretic behavior

The hysteretic curve of Specimen 5 is shown in Fig. 20(a) and that of Specimen 1 is shown in Fig. 20(b). Having Layer 2 with rectangular links made of LYP100, Specimen 5 provided enhanced energy dissipation in terms of ‘fat’ hysteretic loops with nearly no decrease in strength. Meanwhile, notable torsional deformation of double-tapered links in Specimen 1 resulted in pinching in the hysteretic curve. Specimen 5 began to dissipate energy as early as a drift ratio of 0.25%. Equivalent damping ratios estimated using the standard procedure were estimated for each drift ratio (Fig. 20(c)), in which hysteresis of the second cycle was used in the calculation. In the case of Specimen 1, notable torsional deformation occurred at a drift ratio of 2.5%, and accordingly, the damping ratio decreased beyond a drift ratio of 3%. Because of the early yielding and large strain hardening of LYP100, Specimen 5 provided large damping starting from a drift ratio of 1%, which increased to over 0.4 at a drift ratio of 3.5%. Beyond that drift ratio, torsional deformation of the double-tapered links in Layer 1 slightly reduced the equivalent damping ratio yet the ratio remained higher than 0.35 at the completion of loading with a drift ratio of 5%.

Specimen 5 demonstrated the feasibility of realizing structural condition assessment and enhanced energy dissipation simultaneously. The assembly of two layers, one layer with double-tapered links and the other with rectangular links made of low-yield-point steel, formed a workable dual-function system.

8. Effect of bi-directional loading

The foregoing discussion was based on the results under in-plane loading, while bi-directional loading needs be considered in view of practical application. Four cases with different in-plane to out-of-plane loading ratios, i.e., 0, 0.1, 0.5, and 1, were examined numerically under incremental two-cycle loading. Fig. 21 shows the progress of normalized deformation (out-of-plane deformation at the quarter-height section normalized by the plate thickness). As shown in Fig. 21(a), the out-of-plane loading, perpendicular to the plane of double-tapered links, promoted the

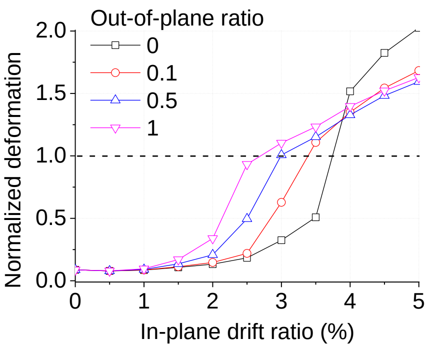

(a)

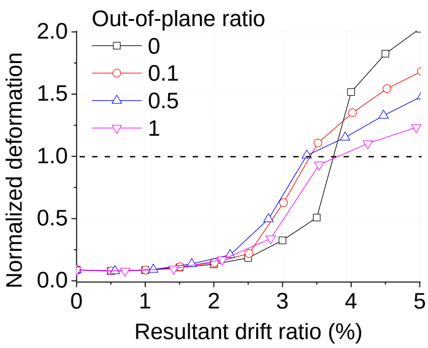

(b)

Fig. 21 Under bi-directional loading: (a) normalized deformation relative to in-plane drift ratio and (b) normalized deformation relative to resultant drift ratio occurrence of notable torsional deformation. The larger the out-of-plane ratio was, the earlier notable torsional deformation was observed. However, the influence remained small when the resultant drift in the two directions was used. In Fig. 21(b), the abscissa is the resultant drift of two components. The link was designed to deform notably at a drift ratio of 4% in-plane deformation. Under bi-directional loading, the link was judged to deform notably at a resultant drift of 3.5%. The difference was regarded to be small. Detailed quantification on the effect of bi-directional loading is a subject of further study.

In practice, the shear wall with double-tapered links may subject to rotation due to beam bending. This accordingly affects the torsional deformation of double-tapered links to some extent. To minimize such influence, pin-supported beams are recommended to the span where the shear wall with double-tapered links is installed such that shear deformation dominates in the behavior of double-tapered links.

9. Conclusions

This paper presented the development of a new type of slit shear wall with double-tapered links that allow condition assessment in post-earthquake inspection of a building's safety. The effectiveness of double-tapered links in assessing the structural condition under various types of loading was investigated, and the feasibility of realizing both structural condition assessment and good energy dissipation was demonstrated by a double-layer system. The major findings obtained in this study are summarized as follows.

• Double-tapered links that were designed with various widths showed notable torsional deformation at drift ratios of 2.5%, 3.5% and 4.5% under the baseline incremental two-cycle loading, clearly supporting the scenario of condition assessment proposed in this study. Torsional deformation of double-tapered links was shown to be stable and repeatable.

• Under earthquake loading, notable torsional deformation of double-tapered links occurred at the largest peak amplitude at which notable torsional deformation was experienced under the baseline incremental two-cycle loading. This indicates that the baseline incremental two-cycle loading is a good representative in determining the occurrence of notable torsional deformation and can thus be adopted in the design of double-tapered links used for condition assessment.

• The addition of an in-plane reference to the double-tapered link improved the objectivity of the inspection of notable torsional deformation with the naked eye. Both the wing-type and whole-height-type references remained in plane throughout the entire loading and provided a good reference for the torsional deformation of double-tapered links.

• Because of the large strain hardening of low-yield-point steel, the slit shear wall with rectangular links made of such steel greatly improved the energy dissipation capacity of the shear wall having double-tapered links. Fracture at the link ends was eliminated using the low-yield-point steel. The assembly of two layers, one having double-tapered links for condition assessment and the other having rectangular links made of low-yield-point steel for energy dissipation, provided a workable dual-function system.

Acknowledgments

The present work is partially supported by the 5th Seismic Isolation and Response-Control research grant award of the Japan Society of Seismic Isolation (PI: Masahiro Kurata). Our sincere thanks go to Dr. Kazuhiro Hayashi and Mr. Takuma Togo for their assistance offered in the experimental work.

References

AISC/AISC 341-05 (2005), *Seismic Provisions For Structural Steel Buildings,* American Institute of Steel Construction, Inc., Chicago.

ATC-24 (1992), *Guidelines For Cyclic Seismic Testing Of Components Of Steel Structures For Buildings*, Report No. ATC-24, Applied Technology Council, Redwood City, CA.

Chan, R.W. and Albermani, F. (2008), "Experimental study of steel slit damper for passive energy dissipation", *Eng. Struct*., **30**(4), 1058-1066.

Chen, S. and Jhang, C. (2006), "Cyclic behavior of low yield strength steel shear walls", *Thin Wall. Struct*., **44**(7), 730-738.

Clark, P., Frank, K., Krawinkler, H. and Shaw, R. (1997), *Protocol For Fabrication, Inspection, Testing, And Documentation Of Beam-Column Connection Tests And Other Experimental Specimens*, SAC Background Document SAC/BD-97/02.

Cortes, G. and Liu, J. (2011), "Experimental evaluation of steel slit panel frames for seismic resistance", *J. Constr. Steel Res.*, **67**(2), 181-191.

Dassault Systèmes (2004), ABAQUS Version 6.10 User's Manual. http://www.abaqus.com

FEMA-461 (2007), *Interim Protocols For Determining Seismic Performance Characteristics Of Structural And Nonstructural Components Through Laboratory Testing,* Federal Emergency Management Agency, Washington.

He, L., Fukihara, K., Kurata, M., Hayashi, H. and Nakashima, M. (2013), "Steel plate shear wall with X-shaped links as a structural component capable of condition assessment", *Proceedings of the Pacific Structural Steel Conference*, Singapore.

Hitaka, T. and Matsui, C. (2003), "Experimental study on steel shear wall with slits", *J. Struct. Eng*., **129**(5), 586-595.

Jacobsen, A. (2010), "Development of steel slit wall dampers with embedded condition assessment capabilities", Ph.D. Dissertation, Kyoto University, Kyoto.

Jacobsen, A., Hitaka, T. and Nakashima, M. (2010), "Online test of building frame with slit wall dampers capable of condition assessment", *J. Constr. Steel Res.*, **66**(11), 1320-1329.

Ke, K. and Chen, Y.Y. (2012), "Design method of steel plate shear wall with slits considering energy dissipation", *Proceedings of the 15th World Conference on Earthquake Engineering*, Lisboa, Portugal.

Kobori, T., Miura, Y., Fukusawa, E., Yamada, T., Arita, T. and Takenake, Y. (1992), "Development and application of hysteresis steel dampers", *Proceedings of the 11th World Conference on Earthquake Engineering, Acapulco,* Mexico.

Kurata, M., He, L. and Nakashiam, M. (2014), "Steel slit shear walls with double-tapered links capable of condition assessment", *Earthq. Eng. Struct. Dyn.*, doi: 10.1002/eqe.2517.

Ma, X., Borchers, E., Peña, A., Krawinkler, H., Billington, S. and Deierlein, G. (2010), *Design And Behavior Of Steel Shear Plates With Openings As Energy-Dissipating Fuses*, John A. Blume Earthquake Engineering Center Technical Report 173. Stanford Digital Repository. http://purl.stanford.edu/hq943jb9995

Nakashima, M. (1995), "Strain-hardening behavior of shear panels made of low-yield steel, I: Test", *J. Struct. Eng*., **121**(12), 1742-1749.

Nakashima, M., Akazawa, T. and Tsuji, B. (1995), "Strain-hardening behavior of shear panels made of low-yield steel, II: Model", *J. Struct. Eng*., **121**(12), 1750-1757.

Nakashima, M., Iwai, S. and Iwata, M. (1994), "Energy dissipation behaviour of shear panels made of low yield steel", *Earthq. Eng. Struct. Dyn.*, **23**(12), 1299-1313.

Okamura, T., Kurata, M., and Nakashima, M. (2012), "Development of slitted steel shear walls capable of detecting damage states", *Proceedings of the 15th World Conference on Earthquake Engineering*, Lisboa, Portugal.
PEER (2009), http://peer.berkeley.edu/transportation/projects/ground-motion-studies-for-transportation-systems/.

JL